
Molecular Mechanics Simulation Studies of Dienoic Hydrocarbons: From Alkenes to 1-Palmitoyl-2-linoleoyl- phosphatidylcholines

SHUSEN LI and CHING-HSIEN HUANG*

Department of Biochemistry, Health Sciences Center, University of Virginia, Charlottesville, Virginia
22908

ABSTRACT

Although no crystal structures of mixed-chain phosphatidylcholines with unsaturated *sn*-2 acyl chains exist, the force field method in conjunction with the experimentally determined structure of saturated identical-chain phosphatidylcholine can be applied to simulate molecular structure for mixed-chain phosphatidylcholines. In this study, the packing models of mixed-chain 1-palmitoyl-2-linoleoyl-phosphatidylcholines in bilayers at temperatures below the gel-liquid crystalline phase transition temperature or $T < T_m$ are simulated by using Allinger's MM3(92) force field. Our results indicate that the unsaturated *sn*-2 acyl chains of the mixed-chain lipid can fold into two energy-minimized topologies: the crankshaftlike and the U-shaped motifs. The folded region in the crankshaftlike *sn*-2 acyl chain is characterized by a sequence $s^-\Delta s^+s^+\Delta s^-$, and the U-shaped chain arises from the characteristic sequence $s^-\Delta s^+s^-\Delta s^+$, where s^\pm denotes the \pm skew conformation and Δ the cis carbon-carbon double bond. These modeled structures of 1-palmitoyl-2-linoleoyl-phosphatidylcholines in the bilayer at $T < T_m$ should not be regarded as highly rigid structures, since torsion angles of carbon-carbon bonds associated with sequences $s^-\Delta s^+s^+\Delta s^-$ and $s^-\Delta s^+s^-\Delta s^+$ can fluctuate somewhat without appreciably affecting the steric energy of the corresponding lipid bilayer. © 1996 by John Wiley & Sons, Inc.

*Author to whom all correspondence should be addressed.

Introduction

Among the various classes of membrane phospholipids, mixed-chain phosphatidylcholines are the most abundant species found in animal cells. The *sn*-1 and *sn*-2 acyl chains of mixed-chain phosphatidylcholines such as 1-palmitoyl-2-linoleoyl-phosphatidylcholine are derived biosynthetically from saturated and unsaturated fatty acyl CoA, respectively. The roles played by mixed-chain phosphatidylcholines in biological membranes have been viewed until recently primarily as those of structural components. This picture has now changed drastically, since many intermediates of the "phosphatidylcholine cycle" are now known to be important signal molecules.^{1,2} In the case of 1-palmitoyl-2-linoleoyl-phosphatidylcholine, for example, one of the breakdown products, linoleic acid, has been implied to play an important role in modulating cellular activities including the G-protein mediated cellular communications.³ Despite the fact that mixed-chain phosphatidylcholines are now known to be important structural and functional molecules in biological membranes, our knowledge of the packing and organization of these lipid molecules in the lipid bilayer is still rather limited. Recently, we established strategies for modeling structures of 1-palmitoyl-2-oleoyl-phosphatidylcholine in bilayers using molecular mechanics calculations.⁴ This strategy is now extended in this study to build the structural models for bilayers comprised of 1-palmitoyl-2-linoleoyl-phosphatidylcholines at temperatures far below the phase transition temperature ($T \ll T_m$).

Materials and Methods

SOFTWARE

The MM3 force field (version 92), originally developed for hydrocarbons by Allinger and co-workers⁵ (supplied by Quantum Chemistry Program Exchange at the Department of Chemistry, Indiana University) was used for our molecular mechanics (MM) force field calculations to simulate the energy-minimized structures and steric energies for hydrocarbons as well as lipid molecules. These calculations were run on an IBM RS/6000 computer workstation. The overall energy function is expressed as steric energy (E_s) by

the MM3 program, and it is composed of various potential energy functions that include primarily bond stretching, bending, torsion, nonbonded van der Waals, dipole-dipole, charge-charge, and bend-bend interactions and other cross-interaction terms such as charge-dipole, stretch-bend, and torsion-stretch. In using Allinger's MM3 program, the hydrogen atoms in $-\text{CH}_2$, $-\text{CH}_3$, and $-\text{CH}=\text{CH}-$ groups within the hydrocarbon or lipid molecules are treated always as individual atoms; this feature is distinctly different from many other computational programs used for proteins or nucleic acids in which the hydrogen atoms are often omitted but added to the bonded carbon atoms to form the so-called united atoms. Moreover, the MM force field used in the MM3 program, originally developed for hydrocarbons, has been shown recently to be capable of accurately describing the structure of the hydrophobic protein crambin.⁶ Allinger's MM3 program is thus employed in the present study for simulating phospholipid molecules in which hydrocarbon chains are, by far, the predominant moieties. However, the MM3 program does not contain force field parameters for the charged phosphate residue, a head-group moiety of the phospholipid molecule. These parameters can be calculated based on published MM2(85) data of analogous compounds.⁷ These calculated values are adjusted with crystallographic data of phospholipids^{8,9} until the calculated internal coordinates of the lipid head group are in reasonably good agreement with experimental data. The main emphasis of this study lies in the structures of the hydrocarbon chains of phospholipid molecules. The force field parameters of the charged phosphate residue are secondary; hence, they are not listed in this communication.

Computer-based molecular graphics were drawn with the software package HyperChem (Hypercube Inc., Waterloo, ON, Canada) performed on a 486 platform. This software package also allows alignments of the graphic images of phospholipid molecules to be made on the screen according to the specific packing mode.

PROCEDURES FOR MOLECULAR MODELING

For each of the hydrocarbon chains under study, an initial crude structure was simply built by forming an extended hydrocarbon conformation using standard bond lengths, bond angles, and torsion angles for the C—C and cis C=C bonds. Subsequently, these initial structures were minimized with the MM3 program. The initial struc-

ture of 1-palmitoyl-2-linoleoyl-phosphatidylcholine, C(16):C(18:2 $\Delta^{9,12}$)PC, was constructed based on the energy-minimized structure of C(16):C(18)PC by replacing the saturated chain segment of C(8)–C(14) in the *sn*-2 acyl chain with the unsaturated C(8)–C(9) = C(10)–C(11)–C(12) = C(13)–C(14) segment. The energy-minimized structure of C(16):C(18)PC was taken from our earlier work.¹⁰ In this initial structure of phosphatidylcholine, the head-group structure was that of the dihydrate of C(14):C(14)PC, structure B, obtained by X-ray diffraction.¹¹ The torsion angles of the initially constructed structure of C(16):C(18:2 $\Delta^{9,12}$)PC were used as a set of input data in obtaining the refined structure of monomeric C(16):C(18:2 $\Delta^{9,12}$)PC using the MM3 programs as described previously.¹² For dimers and tetramers, the MM calculations were performed essentially the same as those described in detail elsewhere.¹⁰

Results

MOLECULAR MODELING OF HYDROCARBON CHAINS CONTAINING TWO CIS DOUBLE BONDS LINKED BY A METHYLENE UNIT

As discussed previously, the presence of a *cis* carbon–carbon double bond (Δ) in a long hydrocarbon chain renders the six atoms in the immediate vicinity of the rigid Δ bond, C—CH=CH—C, coplanar, and this basic planar structure is referred to as the six-atom structural unit.⁴ Moreover, the C—C single bond (σ) either preceding or succeeding the Δ bond is rotationally highly flexible. Based on molecular mechanics MM3 calculations, it was shown that the steric energy profile of the *cis* dodecene-6 resulting from rotations about the C(5)–C(6) single bond (or σ^5 angle) yields two symmetric broad wells ($\pm 80^\circ$ to $\pm 145^\circ$) with the minimal values of torsion angles at $\pm 115^\circ$, corresponding to the C—C bond in the \pm skew(S) conformation.¹³

If a second six-atom structural unit is introduced into a monoenoic hydrocarbon chain in such a way that the two Δ bonds are separated by a methylene unit like the structure of *cis,cis*-2,5-heptadiene, one can expect that the rotational isomers of *cis,cis*-2,5-heptadiene with a set of (σ^3 , σ^4) angles in the neighborhood of 110° (or -110°) will exhibit maximal stability. Now, consider the structures and steric energies of four rotational isomers of *cis,cis*-2,5-heptadiene obtained by Allinger's

MM3 program. These rotational isomers differ only in the values of σ^3 and σ^4 angles as shown in Figure 1. The molecular structure of *cis,cis*-2,5-heptadiene with $\Delta^2 = \Delta^5 = 0^\circ$ and $\sigma^3 = \sigma^4 = 0^\circ$, shown in Figure 1A, is a sterically disallowed conformation with $E_s = 1823.5$ kcal/mol. The rotational isomer with $\Delta^2 = \Delta^5 = 0^\circ$ and $\sigma^3 = \sigma^4 = 65^\circ$ has a more extended conformation with $E_s = 11.0$ kcal/mol (Fig. 1B). The most stable conformation ($E_s = 9.16$ kcal/mol) is found for the rotational isomer with $\Delta^2 = \Delta^5 = 0^\circ$ and $\sigma^3 = \sigma^4 = 110^\circ$ in which the torsional strain and the steric strain from nonbonded interactions with a 1–4 vicinal relationship are at a minimum as shown in Figure 1C. After the MM3 energy minimization, this molecular structure, illustrated in Figure 1C', is refined with $\Delta^2 = 0.7^\circ$, $\sigma^3 = 109.2^\circ$, $\sigma^4 = 109.2^\circ$, $\Delta^5 = 0.7^\circ$, and $E_s = 9.15$ kcal/mol. This refined structure is characterized by a crankshaftlike geometry, and the hydrocarbon sequence around the two Δ bonds can be specified as $\Delta s^+ s^+ \Delta$. The molecular structure of *cis,cis*-2,5-heptadiene with $\Delta^2 = 0^\circ$, $\sigma^3 = 110^\circ$, $\sigma^4 = -110^\circ$, and $\Delta^5 = 0^\circ$ is shown in Figure 1D with $E_s = 9.62$ kcal/mol. After energy minimization, the refined structure is characterized by the following torsion angles: $\Delta^2 = 0.8^\circ$, $\sigma^3 = 110.9^\circ$, $\sigma^4 = -109.7^\circ$, and $\Delta^5 = -0.9^\circ$ with $E_s = 9.30$ kcal/mol. This refined structure with a sequence $\Delta s^+ s^- \Delta$, illustrated in Figure 1D', has a U-shaped geometry.

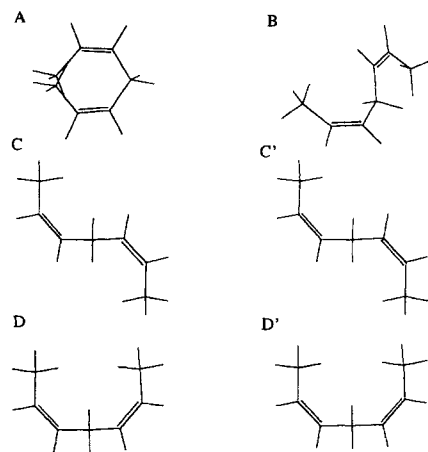


FIGURE 1. Conformations of *cis,cis*-2,5-heptadiene resulting from rotations about the two single C—C bonds (σ^3 , σ^4) located in between the two double bonds (Δ^2 , Δ^5). (A) $\sigma^3 = \sigma^4 = 0^\circ$, (B) $\sigma^3 = \sigma^4 = 65^\circ$, (C) $\sigma^3 = \sigma^4 = 110^\circ$, (C') the refined structure of (C) obtained by the MM3 energy minimization, (D) $\sigma^3 = 110^\circ$, $\sigma^4 = -110^\circ$, (D') the refined structure of (D) obtained by the MM3 energy minimization.

The preferred torsion angles for C—C bonds preceding and succeeding the sequence $\Delta s^+ s^+ \Delta$ can be determined by examining the relationship between the steric energy and the torsion angle for rotations about the C(2)—C(3) bond (σ^2 angle) in *cis,cis*-3,6-nonadiene with a fixed $\Delta s^+ s^+ \Delta$ sequence as shown in Figure 2. Clearly, two broad energy minima centered at torsion angles of $\sigma^2 = \pm 105^\circ$ with $E_s = 9.6$ kcal/mol are observed. When the torsion angles of $\pm 105^\circ$ corresponding to the energy minima are adopted by the C—C single bonds adjacent to the $\Delta s^+ s^+ \Delta$ sequence, the following three sequences can be generated: $s^- \Delta s^+ s^+ \Delta s^-$, $s^- \Delta s^+ s^+ \Delta s^+$, and $s^+ \Delta s^+ s^+ \Delta s^+$.

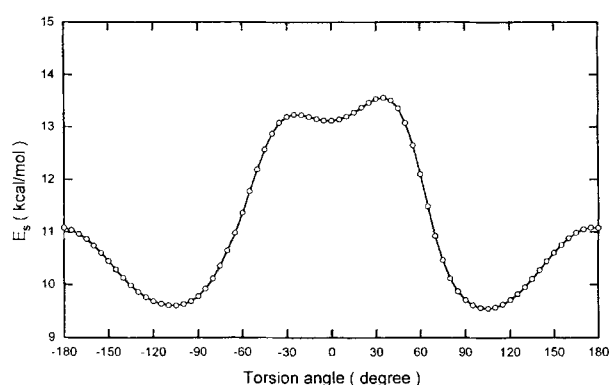


FIGURE 2. The steric energy changes that arise from rotation of the C(2)—C(3) bond (σ^2 angle) of *cis,cis*-3,6-nonadiene. The sequence $\Delta s^+ s^+ \Delta$ is fixed at a set of (0.6°, 107.5°, 109.9°, 0.7°) angles of the σ^2 angle is varied from -180° to $+180^\circ$ in 5° increments.

The torsion angles and the steric energies for rotational isomers of *cis,cis*-5,8-tridecadiene specified by these three sequences, before and after energy minimization, are presented in Table I. Of the three energy-minimized isomers, the one with the sequence $s^- \Delta s^+ s^+ \Delta s^-$ shows the most extended conformation.

DIENOIC HYDROCARBON CHAIN WITH SEQUENCE $s^- \Delta s^+ s^+ \Delta s^-$

The presence of two Δ bonds in a hydrocarbon chain can induce conformational distortions in the hydrocarbon chain. The occurrence of a sequence $s^- \Delta s^+ s^+ \Delta s^-$, however, causes minimal distortions, and the chain is virtually fully extended. Consequently, a dienoic hydrocarbon chain with the sequence $s^- \Delta s^+ s^+ \Delta s^-$ is most likely to prevail in an aggregated structure such as the gel-state bilayer of C(16):C(18:2 $\Delta^{9,12}$)PC. The refined structure of *cis,cis*-5,8-tridecadiene obtained by MM calculations can serve as an example to illustrate the effect of the sequence $s^- \Delta s^+ s^+ \Delta s^-$ on the overall geometry of the hydrocarbon chain. As shown in Figure 3, column 1, this hydrocarbon chain is observed to contain two linear segments. We assign the all-trans zigzag plane of the initial segment as the X-Y (or the paper) plane with the positive X axis being directed toward the right. The positive Z axis runs perpendicularly to the paper plane toward the viewer.

The occurrence of a sequence $s^- \Delta s^+ s^+ \Delta s^-$ near the center of the hydrocarbon chain is seen in

TABLE I. Torsion Angles and Steric Energies for *cis-cis*-5,8-Tridecadiene.

Sequence	Torsion Angle (°)						E_s (kcal/mol)	
	σ^4	Δ^5	σ^6	σ^7	Δ^8	σ^9		
$s^- \Delta s^+ s^+ \Delta s^-$	-105.0	0.7	109.2	109.2	0.7	-105.0	14.02	a
$s^- \Delta s^+ s^+ \Delta s^-$	-105.4	1.0	108.9	109.0	1.0	-105.1	13.60	b
$s^- \Delta s^+ s^+ \Delta s^+$	-105.0	0.7	109.2	109.2	0.7	105.0	13.77	a
$s^- \Delta s^+ s^+ \Delta s^+$	-105.1	1.2	109.0	109.0	0.7	105.4	13.57	b
$s^+ \Delta s^+ s^+ \Delta s^+$	105.0	0.7	109.2	109.2	0.7	105.0	13.93	a
$s^+ \Delta s^+ s^+ \Delta s^+$	105.3	0.8	109.1	109.1	0.8	105.5	13.55	b
$s^+ \Delta s^+ s^- \Delta s^+$	105.0	0.7	109.2	-109.0	0.7	105.0	13.86	a
$s^+ \Delta s^+ s^- \Delta s^+$	105.5	0.6	110.0	-108.7	-0.8	105.8	13.07	b
$s^- \Delta s^+ s^- \Delta s^-$	-105.0	0.7	109.2	-109.0	0.7	-105.0	13.40	a
$s^+ \Delta s^+ s^- \Delta s^-$	-105.7	0.8	110.4	-109.0	-0.6	-105.4	13.07	b
$s^- \Delta s^+ s^- \Delta s^+$	-110.0	0.0	110.0	-110.0	0.0	110.0	47.40	a
$s^- \Delta s^+ s^- \Delta s^+$	-118.7	0.0	112.9	-113.1	0.1	119.5	12.86	b

a: prior to the MM3 energy minimization; b: after MM3 energy minimization.

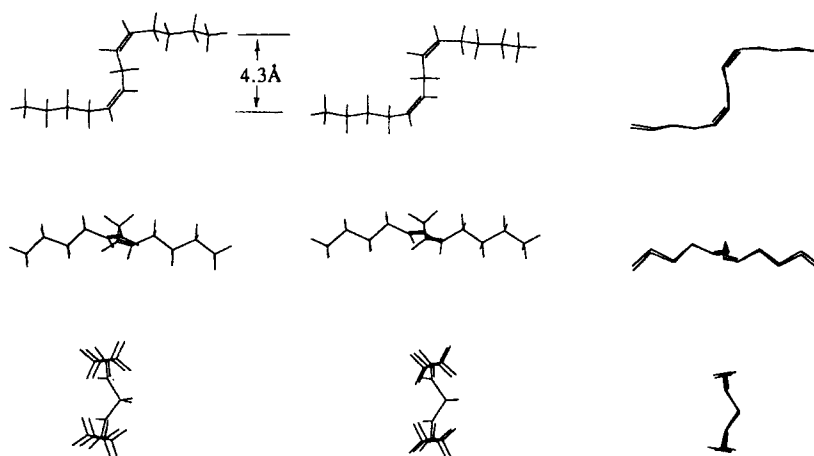


FIGURE 3. Molecular graphics drawings of energy-minimized structures of *cis,cis*-5,8-tridecadiene. Column 1 shows three views of the hydrocarbon chain with the sequences $s^-\Delta s^+s^+\Delta s^-$ obtained by the MM3 force field. Column 2 shows the same hydrocarbon built up initially from crystallographic data of linoleic acid. Column 3 shows the superimposed structures of the two given in columns 1 and 2. Here, the carbon backbone structures are illustrated. In each column, the same hydrocarbon chain is viewed, respectively, on the X-Z plane (top), X-Y plane (middle), and Y-Z plane (bottom).

Figure 3, column 1, to kink the chain into the shape of a crankshaft. Viewed perpendicularly to the X-Z plane, the two linear segments are observed to be nearly parallel, and the averaged vertical distance separating the two linear segments is 4.3 Å along the Z axis (Fig. 3, column 1, top). We can further examine this rotomer by flipping the molecule 90° as shown on the X-Y plane. The two zigzag planes of the two saturated hydrocarbon segments are now seen to be parallel, but not coplanar, with the lower plane extending in front of the zigzag plane of the initial segment (Fig. 3, column 1, middle). Viewed along the C—C axis, the two Δ bonds and the methylene carbon located in between the two Δ bonds are observed to form a V-shaped bridge sandwiched in between the two zigzag planes (Fig. 3, column 1, bottom).

The crystal structure of linoleic acid was determined by X-ray diffraction study, and the torsion angles of the various bonds in the immediate neighborhood of the two Δ bonds in the crystal structure are: $\sigma^8 = -119^\circ$, $\Delta^9 = -2.3^\circ$, $\sigma^{10} = 123^\circ$, $\sigma^{11} = 124^\circ$, $\Delta^{12} = -3.3^\circ$, $\sigma^{13} = -121^\circ$.¹⁴ When these values are used for torsion angles of σ^4 , Δ^5 , σ^6 , σ^7 , Δ^8 , and σ^9 , respectively, in *cis,cis*-5,8-tridecadiene, the molecular structure of the hydrocarbon chain is kinked with a steric energy of 14.66 kcal/mol. Refinements by the MM3 program yield a set of (-110.6° , 0.6° , 117.8° , 110.1° , 0.7° , -110.6°)

angles for the $s^-\Delta s^+s^+\Delta s^-$ sequence with a reduced E value of 13.71 kcal/mol; the resulting structure is shown in Figure 3, column 2 in three orientations. The molecular structure of *cis,cis*-5,8-tridecadiene built up from X-ray diffraction data followed by the MM3 energy minimization can be overlaid on that derived from MM calculations with a root mean square deviation of 0.2 Å only (Fig. 3, column 3).

DIENOIC HYDROCARBON CHAIN WITH SEQUENCE $s^-\Delta s^+s^-\Delta s^+$

The refined structure of *cis,cis*-2,5-heptadiene with a sequence $\Delta s^+s^-\Delta$ was modeled as shown in Figure 1D'. This energy-minimized structure represents another stable conformation of a hydrocarbon chain containing two Δ bonds, and this sequence can thus be used as a basic motif from which other longer unsaturated hydrocarbon chains with stable conformations can be built and refined. Since $\pm S$ configurations correspond to the energy minima for torsion angles of C—C bonds adjacent to the Δ bond, three sequences of $s^+\Delta s^+s^-\Delta s^+$, $s^-\Delta s^+s^-\Delta s^-$, and $s^-\Delta s^+s^-\Delta s^+$ can thus be considered as reasonable candidates for the stable conformations of longer hydrocarbon chains containing a common core motif of $\Delta s^+s^-\Delta$. The structural characteristics of *cis,cis*-5,8-tridecadiene with these three sequences, before and

after the MM3 energy minimization, are presented in Table I. Clearly, the one with a sequence of $s^-\Delta s^+s^-\Delta s^+$ has the lowest E_s value of 12.86 kcal/mol after the MM3 energy minimization (Table I); this structure, shown in Figure 4, is shaped like the letter U. Specifically, the two parallel hydrocarbon segments are separated by 4.3 Å which corresponds closely to the distance between the carbon atoms of the *sn*-1 acyl chain and the zigzag plane of the *sn*-2 acyl chain in the energy-minimized structure of dimyristoyl phosphatidylcholine.¹⁰ It is thus of great interest to expect that such a U-shaped structure may be found in the *sn*-2 acyl chain of phospholipid molecules in the lipid bilayer at $T < T_m$.

MOLECULAR MODELING OF MONOMERIC 1-PALMITOYL-2-LINOLEOYL-PHOSPHATIDYLCHOLINE WITH A COMMON CORE MOTIF OF $\Delta s^+s^+\Delta$ IN *sn*-2 ACYL CHAIN

When the torsion angles of any of the sequences $s^+\Delta s^+s^+\Delta s^+$, $s^-\Delta s^+s^+\Delta s^+$, and $s^-\Delta s^+s^+\Delta s^-$ for energy-minimized *cis,cis*-5,8-tridecadiene shown in Table I are used to replace those of the all-trans C(8)–C(11) segment in the *sn*-2 acyl chain of C(16):C(18)PC, the resulting phospholipid is 1-palmitoyl-2-linoleoyl-phosphatidylcholine or C(16):C(18:2 $\Delta^{9,12}$)PC. It is expected that C(16):C(18:2 $\Delta^{9,12}$)PC containing these sequences in the *sn*-2 acyl chains may have greater stabilities. To search for the most stable form of C(16):C(18:2 $\Delta^{9,12}$)PC with a core motif of $\Delta s^+s^+\Delta$, several rotational isomers of C(16):C(18:2 $\Delta^{9,12}$)PC are initially built from data given in Table I. Furthermore, a structural constraint is imposed on

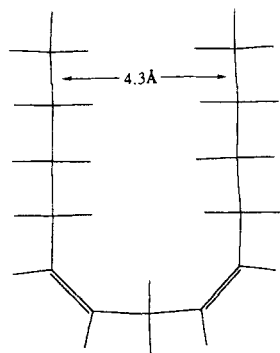


FIGURE 4. Energy-minimized structure of *cis,cis*-5,8-tridecadiene with a sequence $s^-\Delta s^+s^-\Delta s^+$ as viewed on the *X*-*Z* plane.

these initial crude structures of C(16):C(18:2 $\Delta^{9,12}$)PC by assuming the *sn*-1 acyl chain to be in an all-trans conformation, an energetically favorable conformation. The subsequent modeling procedure involves several rounds of energy minimization. In the first round, a crude lipid molecule built up from C(16):C(18)PC and a sequence from Table I is energy minimized with the *sn*-1 acyl chain under restraint as an all-trans acyl chain while the internal coordinates of other moieties are allowed to be modified. In the second round, the resulting structure from round one is refined by allowing the lipid molecule to relax from a geometry with an all-trans *sn*-1 acyl chain. Because the C—C single bonds adjacent to the Δ bond are rotationally flexible with a broad valley of minimum energy centered around $+(105^\circ-120^\circ)$ or $-(105^\circ-120^\circ)$, many conformations with very small differences in E_m (the steric energy for monomeric lipid) are possible. The torsion angles of C—C bonds (σ angles) adjacent to the Δ bonds in the refined structure resulting from round 2 minimization are thus altered slightly ($\leq \pm 5^\circ$), and additional MM calculations are then performed until a minimum in the potential energy surface is practically reached. In this final round of energy minimization, the specific σ angles that are chosen to be altered are guided by molecular graphics but determined by trial and error.

Computational results obtained with C(16):C(18:2 $\Delta^{9,12}$)PC containing sequences $s^+\Delta s^+s^+\Delta s^+$, $s^+\Delta s^+s^+\Delta s^-$, and $s^-\Delta s^+s^+\Delta s^-$, after several rounds of energy minimization, are presented in Table II. In the case of $s^-\Delta s^+s^+\Delta s^-$, the MM derived torsion angles of the sequence based on X-ray crystallographic data of linoleic acid are also summarized in Table II. The molecular graphics representations of these rotational isomers are illustrated in Figure 5.

If the zigzag plane of the *sn*-1 acyl chain is assigned as the *X*-*Y* plane of the lipid structure with the positive *X* axis pointing toward the methyl end, the chain axes of the two segments of the *sn*-2 acyl chain (illustrated in Fig. 5A), are seen to align nearly perpendicularly to each other on the *X*-*Y* plane for C(16):C(18:2 $\Delta^{9,12}$)PC with a sequence $s^+\Delta s^+s^+\Delta s^+$. In this case, the van der Waals favorable interactions between the *sn*-1 and *sn*-2 acyl chains are limited to the upper half of the lipid molecule, resulting in a relatively larger value of 7.18 kcal/mol for E_m . For C(16):C(18:2 $\Delta^{9,12}$)PC with a sequence $s^-\Delta s^+s^+\Delta s^+$, the chain axis of the initial linear segment of the *sn*-2 acyl chain is seen on the *X*-*Y* plane to run in parallel with the

TABLE II.

Torsion Angles and Steric Energies for Monomeric C(16):C(18: $\Delta^{9,12}$)PC with Various Sequences in *sn*-2 Acyl Chain after MM3 Energy Minimization.

Sequence	Torsion Angle ($^{\circ}$)						E_m (kcal/mol)
	σ^4	Δ^5	σ^6	σ^7	Δ^8	σ^9	
$s^+\Delta s^+\Delta s^+$	105.0	0.7	107.9	109.5	0.7	105.7	7.18
$s^-\Delta s^+\Delta s^+$	-101.6	1.3	111.7	105.7	1.3	115.6	3.96
$s^-\Delta s^+\Delta s^+$	-142.5	-1.3	109.3	92.5	0.3	114.0	5.96
$s^-\Delta s^+\Delta s^-^a$	-107.1	1.0	129.1	117.9	1.1	-114.8	3.58
$s^-\Delta s^+\Delta s^-$	-101.5	0.8	127.3	115.6	0.8	-114.0	3.95
$s^-\Delta s^+\Delta s^-$	-105.8	1.6	121.1	110.0	0.7	-110.0	4.32
$s^-\Delta s^+\Delta s^-$	-94.6	1.3	126.3	-120.8	-1.2	-109.7	5.00
$s^+\Delta s^+\Delta s^+$	108.5	0.6	110.2	-104.9	-0.7	100.5	5.20
$s^-\Delta s^+\Delta s^+$	-110.1	0.4	123.6	-107.9	-0.4	117.9	1.99
$s^-\Delta s^+\Delta s^+$	-104.8	0.4	125.5	-111.5	-0.4	118.5	1.73

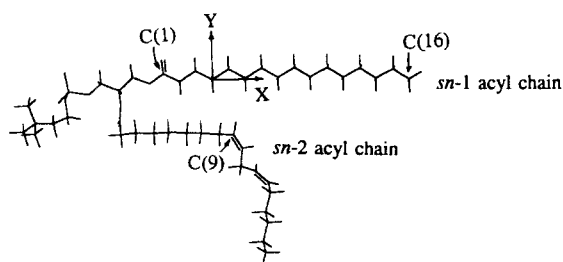
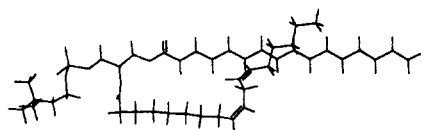
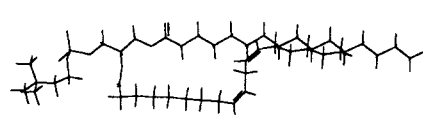
^aThe initial values of torsion angles were taken from crystallographic data of linoleic acid.¹⁴A. With a sequence $s^+\Delta s^+\Delta s^+$ in the *sn*-2 acyl chainB. With a sequence $s^-\Delta s^+\Delta s^+$ in the *sn*-2 acyl chainC. With a sequence $s^-\Delta s^+\Delta s^-$ in the *sn*-2 acyl chain

FIGURE 5. Energy-minimized structures of 1-palmitoyl-2-linoleoyl-phosphatidylcholine with various sequences in the *sn*-2 acyl chains. The structures shown in (A), (B), and (C) have, respectively, sequences $s^+\Delta s^+\Delta s^+$, $s^-\Delta s^+\Delta s^+$, and $s^-\Delta s^+\Delta s^-$.

long chain axis of the *sn*-1 acyl chain (Fig. 5B). The lower linear segment of the *sn*-2 acyl chain is canted on the X-Y plane with the terminal methyl group lying above and in front of the *sn*-1 acyl chain as shown in Figure 5B. The steric energy for this isomer fluctuates from 3.96 to 5.96 kcal/mol

as shown in Table II. Finally, let us consider the structural characteristics of C(16):C(18:2 $\Delta^{9,12}$)PC with a sequence $s^-\Delta s^+\Delta s^-$ in the *sn*-2 acyl chain as illustrated in Figure 5C. The *sn*-2 acyl chain of this rotational isomer exhibits a crankshaftlike conformation. Specifically, the upper segment of the *sn*-2 acyl chain lies underneath (at -Y direction) and in front of (at +Z direction) the *sn*-1 acyl chain with favorable van der Waals attractive distance between them. In contrast, the lower segment of the *sn*-2 acyl chain lies nearly perfectly in front of the *sn*-1 acyl chain. This rotomer of C(16):C(18:2 $\Delta^{9,12}$)PC has E_m value of 3.95 kcal/mol. It should be emphasized that the structure of C(16):C(18:2 $\Delta^{9,12}$)PC with a sequence $s^-\Delta s^+\Delta s^-$ shown in Figure 5C represents only one of several optimal conformations, including the one built up from X-ray diffraction data. These optimal conformations with a common sequence of $s^-\Delta s^+\Delta s^-$ are listed in Table II; they all have nearly identical values of E_m ranging from 3.58 to 4.32 kcal/mol. Hence, structural fluctuations, in terms of torsion angles, do exist, although these isomers have the same overall crankshaftlike topology. These fluctuations imply that the modeled structure of C(16):C(18:2 $\Delta^{9,12}$)PC with a crankshaftlike *sn*-2 acyl chain is not highly rigid, but rather flexible.

MOLECULAR MODELING OF MONOMERIC C(16):C(18:2 $\Delta^{9,12}$)PC WITH A COMMON CORE MOTIF OF $\Delta s^+s^-\Delta$ IN *sn*-2 ACYL CHAIN

After the torsion angles of sequences $s^+\Delta s^+s^-\Delta s^+$, $s^-\Delta s^+s^-\Delta s^-$, and $s^-\Delta s^+s^-\Delta s^+$ in

the energy-minimized structures of *cis,cis*-5,8-tridecadiene (shown in Table I) were employed as the initial coordinates to build the molecular structures of C(16):C(18:2 $\Delta^{9,12}$)PC by the MM approach, three optimal conformations were obtained as illustrated graphically in Figure 6. The values of several sets of ($\sigma^8, \Delta^9, \sigma^{10}, \sigma^{11}, \Delta^{12}, \sigma^{13}$) angles associated with these conformations are summarized in Table II. For C(16):C(18:2 $\Delta^{9,12}$)PC with a sequence $s^-\Delta s^+s^-\Delta s^-$, the bent *sn*-2 acyl chain resembles the shape of a tilted letter V as the *X*-*Y* plane of the lipid molecule lies in the paper plane (Fig. 6A); the E_m value is 5.0 kcal/mol. In the case of C(16):C(18:2 $\Delta^{9,12}$)PC with a sequence of $s^+\Delta s^+s^-\Delta s^+$, the *sn*-2 acyl chain also bends sharply at the bridge ($\Delta s^+s^-\Delta$) region when viewed perpendicularly to the *X*-*Y* plane (Fig. 6B). The E_m value of this energy-minimized structure is 5.2 kcal/mol. The most stable conformation of C(16):C(18:2 $\Delta^{9,12}$)PC with a core motif of $\Delta s^+s^-\Delta$ is the one with a U-shaped *sn*-2 acyl chain ($E_s = 1.73$ kcal/mol) characterized by the sequence $s^-\Delta s^+s^-\Delta s^+$ as shown in Table II. Viewed perpendicularly to the *X*-*Y* plane, the

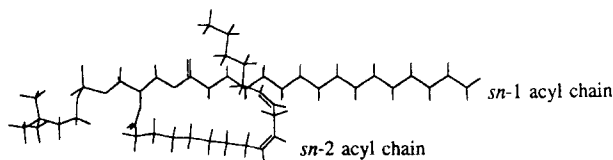
two linear segments of the *sn*-2 acyl chain of this lipid molecule (see Fig. 6C) run in an antiparallel manner. The separation distance between the non-bonded C(5) and C(16) atoms in the U-shaped *sn*-2 acyl chain is 4.3 Å. In this same view, the lower linear segment of the *sn*-2 acyl chain is extended in front of the zigzag plane of the *sn*-1 acyl chain with a separation distance of 4.2 Å along the *Z* axis between the chain axis of the lower segment and the zigzag plane of the *sn*-1 acyl chain.

INTERCONVERSION OF CONFORMATIONS OF *sn*-2 ACYL CHAIN IN C(16):C(18:2 $\Delta^{9,12}$)PC BETWEEN CRANKSHAFT- AND U-SHAPED TOPOLOGY

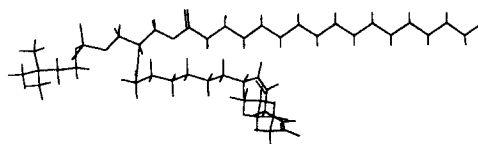
Based on steric energy calculations, monomeric C(16):C(18:2 $\Delta^{9,12}$)PC with a crankshaftlike *sn*-2 acyl chain can be regarded as the most stable conformation among all rotational isomers with a common core motif of $\Delta s^+s^+\Delta$. Similarly, the same lipid with a U-shaped *sn*-2 acyl chain is the most stable conformation for all isomers with a common core motif of $\Delta s^+s^-\Delta$. The steric energy difference (ΔE_m) between these two stable conformations is about 2.22 kcal/mol. If we consider only these two conformations, then at -20°C , about 98.8% of the *sn*-2 acyl chain in C(16):C(18:2 $\Delta^{9,12}$)PC should be in the U-shaped topology.

Structurally, the U-shaped *sn*-2 acyl chain can be considered simply as a variation of the crankshaftlike topology and vice versa. In this sense, these two conformations can be interconverted by reversing the orientation of the lower segment of the *sn*-2 acyl chain. This reorientation can be accomplished by rotating simultaneously about the two C—C single bonds adjacent to the Δ^{12} bond, or the set of (σ^{11}, σ^{13})-torsion angles, from the s^+/s^- to the s^-/s^+ values. As the (σ^{11}, σ^{13}) angles reverse their signs simultaneously, the largest energy barrier for rotations occurs at $\sigma^{11} = \sigma^{13} = 180^\circ$. It can be estimated by MM calculations that the rotational barrier is about 4.41 kcal/mol as the *sn*-2 acyl chain is going from the crankshaft- to the U-shaped geometry, with the set of (σ^{11}, σ^{13}) angles converting from ($115.6^\circ, -114^\circ$) to ($-108.0^\circ, 118^\circ$). This barrier is raised to 6.60 kcal/mol for the reversed conversion. The results of our simple calculations merely point out the possibility that once C(16):C(18:2 $\Delta^{9,12}$)PC molecules adopt the crankshaft conformation at $T < T_m$, they may be trapped kinetically in this conformation. This is due to the facts that not only a kinetic barrier exists between the

A. With a sequence $s^-\Delta s^+s^-\Delta s^-$ in the *sn*-2 acyl chain



B. With a sequence $s^+\Delta s^+s^-\Delta s^+$ in the *sn*-2 acyl chain



C. With a sequence $s^-\Delta s^+s^-\Delta s^+$ in the *sn*-2 acyl chain

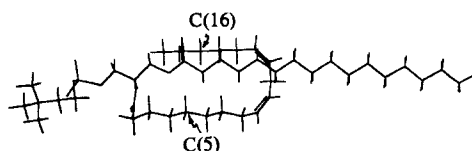


FIGURE 6. Energy-minimized structures of 1-palmitoyl-2-linoleoyl-phosphatidylcholines with various sequences in the *sn*-2 acyl chains: (A) $s^+\Delta s^+s^-\Delta s^-$, (B) $s^+\Delta s^+s^-\Delta s^+$, and (C) $s^-\Delta s^+s^-\Delta s^+$.

two conformations (crankshaft and U-shaped), but also the probability of having two C—C bonds to undergo opposite rotations at the same time, a process which is essential for the conversion to take place successfully, is scarce.

MM SIMULATIONS OF DIMERIC AND TETRAMERIC C(16):C(18:2 $\Delta^{9,12}$)PC WITH CRANKSHAFT- AND U-SHAPED *sn*-2 ACYL CHAINS

We now turn to examine the energy-minimized structures of dimeric C(16):C(18:2 $\Delta^{9,12}$)PC modeled in the trans-bilayer motif with twofold symmetry. In this trans-bilayer dimer, the hydrocarbon chains of one lipid are packed against the opposing hydrocarbon chains of another lipid to form a hydrocarbon core which, in turn, is sandwiched in between the two polar head groups of the dimeric phospholipids.

As a first example, consider C(16):C(18:2 $\Delta^{9,12}$)PC with a crankshaftlike *sn*-2 acyl chain. Two energy-minimized structures of C(16):C(18:2 $\Delta^{9,12}$)PC were aligned on the computer screen in such a manner that the terminal methyl groups of the *sn*-1 and *sn*-2 acyl chains of one lipid molecule were arranged face to face with those of the *sn*-2 and *sn*-1 acyl chains, respectively, of another lipid molecule. Furthermore, these two pairs of methyl groups were separated by 4.1 Å. After the alignment, the

dimer was then subjected to MM3 energy minimization. The resulting model of dimeric C(16):C(18:2 $\Delta^{9,12}$)PC is presented in Figure 7A. In this trans-bilayer dimer, the distance between the two carbonyl oxygens in the two all-trans *sn*-1 acyl chains, along the X axis, is 37.6 Å, corresponding to the thickness of the hydrocarbon core within the trans-bilayer dimer. The separation distances between the two pairs of terminal methyl groups are 4.2 Å. Laterally, the nonbonded carbon-carbon distance between the two adjacent C(15) atoms in the two fully extended *sn*-1 acyl chains is 4.3 Å. Intramolecularly, the closest nonbonded C—C contact distance (4.0 Å) occurs between the C(6) of the *sn*-1 acyl chain and C(11) of the *sn*-2 acyl chain. The steric energy, E_d^C , is 6.11 kcal/mol. Here, the superscript C in the steric energy term denotes the crankshaftlike topology of the *sn*-2 acyl chain and the subscript d refers to the dimeric model. The stabilization energy of association of the trans-bilayer dimer contributed by each monomer, ΔE_d^C , can be calculated as follows: $\Delta E_d^C = (E_d^C - 2E_m^C)/2 = (6.11 - 2 \times 3.95)/2 = -0.90$ kcal/mol, where E_m^C is the steric energy for monomeric C(16):C(18:2 $\Delta^{9,12}$)PC with a crankshaftlike *sn*-2 acyl chain.

The trans-bilayer dimer shown in Figure 7A can be employed as the parent structure to construct two types of tetramer. Figure 7B shows the

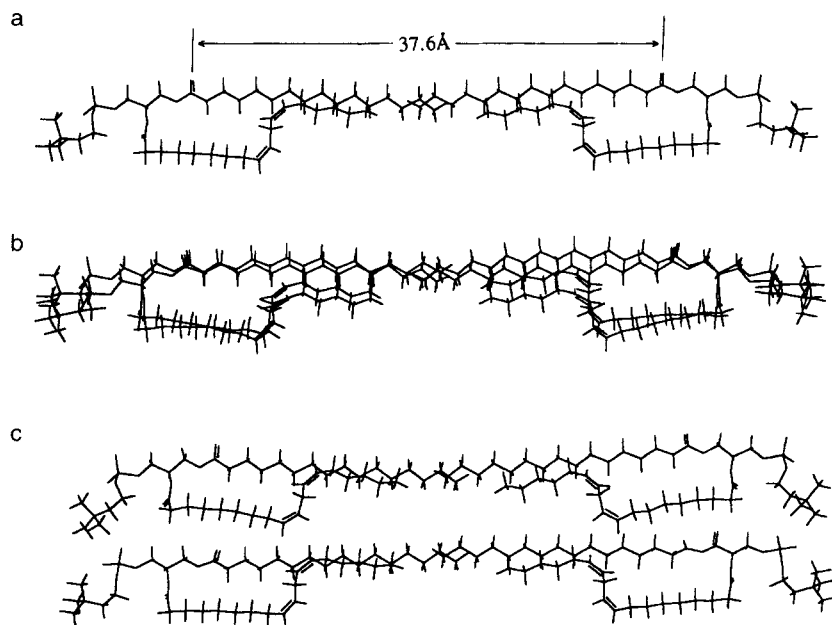


FIGURE 7. Trans-bilayer dimer and dimer of trans-bilayer dimers of 1-palmitoyl-2-linoleoyl-phosphatidylcholines with crankshaftlike *sn*-2 acyl chains: (A) trans-bilayer dimer, (B) F-B tetramer, and (C) U-D tetramer.

energy-minimized structure of the juxtaposition of two such trans-bilayer dimers called the front to back (F-B) tetramer. This F-B tetramer is characterized by the superposition of two trans-bilayer dimers stacked in an eclipsed position, allowing the X-Y plane of one dimer to be parallel to the X-Y plane of the other trans-bilayer dimer. The steric energy, $E_t^{C,F-B}$, of this tetramer obtained from MM calculations is -36.77 kcal/mol. The superscript F-B used in the steric energy term refers to the F-B packing motif and the subscript t denotes the tetramer. The stabilization energy of association of the tetramer contributed by each monomer can be calculated as follows: $\Delta E_t^{C,F-B} = (E_t^{C,F-B} - 4E_m^C)/4 = -13.14$ kcal/mol.

Figure 7C illustrates the energy-minimized structure of a second type of tetrameric C(16):C(18:2 $\Delta^{9,12}$)PC. In this second packing motif, two trans-bilayer dimers are aligned side by side such that the X-Y planes of the two adjacent trans-bilayer dimers are coplanar. We refer to this packing motif as the up and down (U-D) motif. The steric energy of this U-D tetramer, $E_t^{C,U-D} = -35.37$ kcal/mol, can be used to calculate the stabilization energy of association contributed by the monomer ($\Delta E_t^{C,U-D}$), yielding a value of -12.79 kcal/mol for $\Delta E_t^{C,U-D}$. If two tetramers, one with the F-B motif and the other with the U-D motif, are closely packed to mimic, to a first approximation, the orthorhombic 2-dimensional structures of phospholipids assembled in the lipid bilayer at $T < T_m$, the overall averaged stabilization energy ($\Delta E_t^{C,ave}$) can then be derived from the sum of the ΔE_t^C values for the two types of tetramers as follows: $\Delta E_t^{C,ave} = 1/2(\Delta E_t^{C,F-B} + \Delta E_t^{C,U-D}) = -12.97$ kcal/mol. Although this calculated value by itself is not of any great significance, it is useful when comparing with the similar term, $\Delta E_t^{U,ave}$, for two tetrameric C(16):C(18:2 $\Delta^{9,12}$)PC with U-shaped *sn*-2 acyl chains packed in an orthorhombic lattice. This point will become clear later.

Now, we can proceed to show the various oligomers of C(16):C(18:2 $\Delta^{9,12}$)PC with U-shaped *sn*-2 acyl chains. It is worth pointing out that the main characteristic feature of a C(16):C(18:2 $\Delta^{9,12}$)PC molecule with a U-shaped *sn*-2 acyl chain is that the effective *sn*-1 acyl chain length is about twice as long as the effective chain length of the folded *sn*-2 acyl chain. In forming the trans-bilayer dimer, the folded *sn*-2 acyl chain of one lipid molecule is packed against the same U-shaped *sn*-2 acyl chain from the opposing lipid molecule so that the two looped regions are positioned near

the center of the trans-bilayer dimer. In this packing motif, the two all-trans *sn*-1 acyl chains of a trans-bilayer dimer are coplanar, and each effective *sn*-1 acyl chain length matches nearly perfectly with the sum of two folded *sn*-2 acyl chains. Consequently, the chain-chain interactions in this trans-bilayer dimer are optimal. Viewing the dimeric model on the X-Y plane, the two *sn*-1 acyl chains form a layer of hydrocarbon chains, which is called face I. The two U-shaped *sn*-2 acyl chains are also coplanar in the same view down along the negative Z axis. These planar chains lie on top of face I, forming the second layer of hydrocarbon chains called face II. However, the zigzag plane of the saturated hydrocarbon segment in face II is oriented perpendicularly to that in face I. An energy-minimized structure of the trans-bilayer dimeric C(16):C(18:2 $\Delta^{9,12}$)PC with U-shaped *sn*-2 acyl chains, obtained with the MM3 program, is shown in Figure 8A. The averaged separation distance between the chain axis of the saturated segment of the hydrocarbon chain in face II and the zigzag plane of the fully extended *sn*-1 acyl chain in face I is 4.2 Å. The separation distance between the two carbonyl oxygens in the opposing *sn*-1 acyl chain is 16.8 Å. A distance of 4.0 Å is obtained near the trans-bilayer center

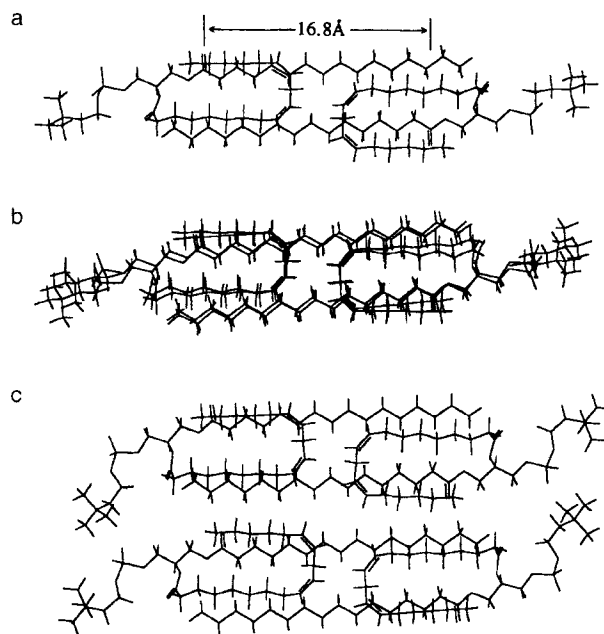


FIGURE 8. Trans-bilayer dimer and dimer of trans-bilayer dimers of 1-palmitoyl-2-linoleoyl-phosphatidylcholines with U-shaped *sn*-2 acyl chains: (A) trans-bilayer dimer, (B) F-B tetramer, and (C) U-D tetramer.

between the two C(10) atoms in the two opposing *sn*-2 acyl chains. This energy-minimized dimer has a steric energy (E_d^U) of -12.82 kcal/mol. The stabilization energy of association of the dimer contributed by each monomer, ΔE_d^U , is thus -8.14 kcal/mol.

When a trans-bilayer dimer of C(16):C(18:2 $\Delta^{9,12}$)PC with U-shaped *sn*-2 acyl chains is used as the parent structure to construct the F-B and U-D tetramers, five different pairs of interfaces can be formed in a dimer of trans-bilayer dimers. In the case of F-B tetramers, three different pairs of interfaces (face I-face I, face I-face II, face II-face II) can be formed and they each have distinct strength, reflected in their stabilization energy of association contributed by the monomer ($\Delta E_t^{U,F-B}$). MM calculations indicate that a tetramer with the face I-face II interface has a $\Delta E_t^{U,F-B}$ value of -22.16 kcal/mol, which is slightly smaller than the averaged $\Delta E_t^{U,F-B}$ value (-22.09 kcal/mol) calculated for a pair of tetramers with face I-face I and face II-face II interfaces. The energy-minimized dimer of trans-bilayer dimers with a face I-face II interface is illustrated in Figure 8B. It has a steric energy, $E_t^{U,F-B}$, of -81.72 kcal/mol. In this structure, the terminal segments of both *sn*-1 acyl chains are flattened somewhat at the face I-face II interface. Moreover, the separation distances along the Z axis between the two C(13)-C(18) segments of the *sn*-1 acyl chains from one trans-bilayer dimer and the two C(2)-C(9) segments of the *sn*-2 acyl chains from the other trans-bilayer dimer are 4.3 – 4.4 Å at the interface, indicating that the two trans-bilayer dimers are held together in the dimer of dimers primarily by favorable van der Waals interactions between face I and face II of each dimeric C(16):C(18:2 $\Delta^{9,12}$)PC.

When two trans-bilayer dimers are aligned side by side to form the U-D tetramer, two different pairs of interfaces can be formed as indicated by the dotted lines as follows: (face I/face II \cdots face I/face II) and (face I/face II \cdots face II/face I). Of these two U-D dimers of dimers, the one with (face I/face II \cdots face I/face II) interface has $E_t^{U,U-D}$ of -81.18 kcal/mol. In contrast, the other one has $E_t^{U,U-D}$ of -40.64 kcal/mol. The energy-minimized structure of the dimer of trans-bilayer dimers with $E_t^{U,U-D}$ of -81.18 kcal/mol is presented in Figure 8C. In this structure, the separation distances between the two pairs of *sn*-2 chain axes at the interface are 4.3 – 4.4 Å. The nonbonded carbon-carbon distances between C(7), C(9) of one *sn*-1 acyl chain and C(9), C(7) of the adjacent *sn*-1 acyl chain are equal, 4.0 Å, at the interface within

the U-D tetramer. The stabilization energy of association calculated for this U-D tetramer is -22.03 kcal/mol, which is virtually identical to that (-22.16 kcal/mol) calculated for the F-B tetramer. The averaged overall stabilization, $\Delta E_t^{U,ave}$, can be taken as a mean value of the two tetramers as follows: $\Delta E_t^{U,ave} = 1/2(\Delta E_t^{U,F-B} + \Delta E_t^{U,U-D}) = -22.10$ kcal/mol. This value is 9.13 kcal/mol smaller than that calculated for $\Delta E_t^{C,ave}$, indicating that oligomers of C(16):C(18:1 $\Delta^{9,12}$)PC with U-shaped *sn*-2 acyl chains are packed more favorably in an orthorhombic lattice than those comprised of the same lipids with crankshaftlike *sn*-2 acyl chains.

Discussion

Although the crystal structures of many membrane lipids have been determined by X-ray diffraction techniques,¹⁵ those of naturally occurring mixed-chain phosphatidylcholines in which the *sn*-1 and *sn*-2 acyl chains contain saturated and unsaturated hydrocarbons, respectively, remain largely unknown. In this communication, we have applied the computational method to model the monomeric and oligomeric structures of C(16):C(18:2 $\Delta^{9,12}$)PC. Our MM3 computations first demonstrated that hydrocarbon chains with two Δ bonds separated by a methylene unit would exhibit minimal steric energies when the C—C single bonds adjacent to the Δ bonds were rotated into the S ($\pm 105^\circ$ to $\pm 120^\circ$) conformation. In fact, two groups of hydrocarbon chains with core sequences of $\Delta s^+ s^+ \Delta$ and $\Delta s^+ s^- \Delta$ were constructed. MM calculations reveal that hydrocarbon structures with sequences $s^- \Delta s^+ s^+ \Delta s^-$ and $s^- \Delta s^+ s^- \Delta s^+$ have distinctly higher stabilities. With a sequence $s^- \Delta s^+ s^+ \Delta s^-$, the dienoic hydrocarbon can give rise to a crankshaftlike motif. Most interestingly, this motif and the one built up from the crystallographic data of linoleic acid are strikingly similar (Fig. 3), lending strong support to the computational method used in this study as a reasonably viable approach.

Our computational models of C(16):C(18:2 $\Delta^{9,12}$)PC were constructed initially by aligning the region around the two Δ bonds in the *sn*-2 acyl chain in congruence with the corresponding region of a long dienoic hydrocarbon chain. As discussed earlier, two conformations of an isolated dienoic chain with sequences $s^- \Delta s^+ s^+ \Delta s^-$ and $s^- \Delta s^+ s^- \Delta s^+$ were identified as the most stable

forms. Consequently, two models for monomeric C(16):C(18:2 $\Delta^{9,12}$)PC were also established by the MM method. The most prominent features of these two models are the crankshaftlike and U-shaped topologies of the *sn*-2 acyl chains. Moreover, within each model the van der Waals contact interactions between the *sn*-1 and *sn*-2 acyl chains in C(16):C(18:2 $\Delta^{9,12}$)PC were optimal. Based on these crankshaft- and U-shaped motifs, the trans-bilayer dimers and oligomers of C(16):C(18:2 $\Delta^{9,12}$)PC were also modeled. These oligomers were taken, to a first approximation, as the lipid bilayer model comprised of C(16):C(18:2 $\Delta^{9,12}$)PC.

The bilayer model built up from C(16):C(18:2 $\Delta^{9,12}$)PC with U-shaped *sn*-2 acyl chains deviated considerably from either the conventional or the mixed interdigitated gel-state bilayer.¹⁶ This new bilayer model is unique in two respects (Fig. 8). First, each trans-bilayer dimer has two layers (face I and face II) of hydrocarbon chains. Second, all terminal methyl groups in the *sn*-1 and *sn*-2 acyl chains are positioned near the head-group/hydrocarbon interfaces. In the future, experimental tests to validate this novel bilayer model for C(16):C(18:2 $\Delta^{9,12}$)PC should be a rewarding enterprise.

The second bilayer model of C(16):C(18:2 $\Delta^{9,12}$)PC with crankshaftlike *sn*-2 acyl chains is shown in Figure 7. The overall average stabilization energy of this bilayer model is -12.97 kcal/mol. This ΔE_t^{ave} value is larger than the ΔE_t^{ave} value (-16.11 kcal/mol) calculated for C(16):C(18:1 Δ^9)PC which, in turn, is larger than that (-16.92 kcal/mol) calculated for C(16):C(18)PC. This trend reflects the order of stability of these three bilayer models as follows: C(16):C(18)PC > C(16):C(18:1 Δ^9)PC > C(16):C(18:2 $\Delta^{9,12}$)PC. It is well established from calorimetric studies that the T_m and ΔH values associated with the gel-liquid crystalline phase transition for lipid bilayers, prepared from phosphatidylcholines containing the same number of total carbon atoms, depend on the number of Δ bonds in their acyl chains.^{17,18} For instance, the T_m values for bilayers prepared from C(18):C(18)PC, C(18):C(18:1 Δ^9)PC, and C(18):C(18:2 $\Delta^{9,12}$)PC are 55.7, 5.6, and -14.6°C , respectively.^{12,19,20} This progressive decrease in T_m reflects the trend of relative stability of these lipid bilayers at $T < T_m$. The

order of ΔE_t^{ave} values calculated for C(16):C(18)PC, C(16):C(18:1 Δ^9)PC, and C(16):C(18:2 $\Delta^{9,12}$)PC, which also reflects the relative stability, is thus in complete accord with the chain melting behavior exhibited by similar bilayer systems. Consequently, the modeled crankshaftlike *sn*-2 acyl chain can be taken as a plausible motif for the *sn*-2 acyl chain of C(16):C(18:2 $\Delta^{9,12}$)PC packed in the bilayer at $T < T_m$.

Acknowledgments

This research was supported in part by NIH Grant GM-17452 to C.H.

References

1. J. H. Exton, *Biochim. Biophys. Acta*, **1212**, 26 (1994).
2. H. Tronchere, M. Record, F. Terce, and H. Chap, *Biochim. Biophys. Acta*, **1212**, 831 (1994).
3. H. S. Hansen, *Trends Biochem. Sci.*, **18**, 164 (1993).
4. S. Li, H. Lin, Z. Wang, and C. Huang, *Biophys. J.*, **66**, 2005 (1994).
5. N. L. Allinger, Y. H. Yuh, and J-H. Lii, *J. Am. Chem. Soc.*, **111**, 8551 (1989).
6. J-H. Lii and N. L. Allinger, *J. Comp. Chem.*, **12**, 186 (1991).
7. S. Li, Z. Cheng, and C. Yuan, *Sci. China*, **32B**, 1172 (1989).
8. I. Pascher and S. Sundell, *Biochim. Biophys. Acta*, **855**, 68 (1986).
9. I. Pascher, S. Sundell, K. Harlos, and H. Ebl, *Biochim. Biophys. Acta*, **896**, 77 (1987).
10. S. Li, Z. Wang, H. Lin, and C. Huang, *Biophys. J.*, **65**, 1415 (1993).
11. R. H. Pearson and I. Pascher, *Nature*, **281**, 499 (1979).
12. Z. Wang, H. Lin, S. Li, and C. Huang, *J. Biol. Chem.*, **270**, 2014 (1995).
13. C. Huang and S. Li, In *Nonmedical Applications of Liposomes*, Y. Barenholz and D. D. Lasic, Eds., CRC Press, Boca Raton, FL, 1996, chap. 7.
14. J. Ernst, W. S. Sheldick, and J-H. Fuhrhop, *Z. Naturforsch.*, **34b**, 706 (1979).
15. I. Pascher, M. Lundmark, P-G. Nyholm, and S. Sundell, *Biochim. Biophys. Acta*, **1113**, 339 (1992).
16. C. Huang, *Klin. Wochenschr.*, **68**, 149 (1990).
17. K. P. Coolbear, C. B. Berde, and K. M. W. Keough, *Biochemistry*, **22**, 1466 (1983).
18. K. M. W. Keough, B. Griffin, and N. Kariel, *Biochim. Biophys. Acta*, **902**, 1 (1987).
19. C. Huang, S. Li, Z. Wang, and H. Lin, *Lipids*, **28**, 365 (1993).
20. C. D. Niebylski and N. Salem, *Biophys. J.*, **67**, 2387 (1994).